BMC Cancer

RESEARCH Open Access

The lncRNA *AFAP1-AS1* is upregulated in metastatic triple-negative breast tumors and controls hypoxia-activated vasculogenic mimicry and angiogenesis

Alejandra Paola García-Hernández[1], David Núñez Corona[1], Ángeles Carlos-Reyes[2], Mónica Sierra-Martínez[3], Gustavo Acosta-Altamirano[4], Mireya Cisneros-Villanueva[5], Yussel Pérez-Navarro[1], Eloisa Ibarra-Sierra[6], Laurence A. Marchat[7] and César López-Camarillo[1*]

Abstract

Background Vasculogenic mimicry (VM) is an alternative intratumoral microcirculation system that depends on the capacity of tumor cells to reorganize and grow in three-dimensional (3D) channel architectures like the capillaries formed by endothelial cells. Both VM and angiogenesis may coordinately function to feed cancer cells, allowing tumor growth. Long noncoding RNAs (lncRNAs) regulate critical cellular functions in cancer cells, including cell proliferation, apoptosis, angiogenesis, invasion, and metastasis. The lncRNA, known as actin filament-associated protein 1-antisense RNA 1 (*AFAP1-AS1*), has been described as an oncogene in diverse types of cancers. However, its role in VM and metastasis in triple-negative breast cancer (TNBC) is unknown.

Methods Reverse transcription and quantitative polymerase chain reaction (RT–qPCR) experiments were performed to evaluate the expression of 10 selected lncRNAs from literature in metastatic and nonmetastatic biopsies from TNBC patients. The expression of *AFAP1-AS1* was analyzed in Genotype-Tissue Expression Genotype-Tissue Expression (GTEx) and The Cancer Genome Atlas (TCGA) datasets. The *AFAP1-AS1* expression was knocked in TNBC Hs578T cells by transfection of specific siRNAs. Channel-like formation assays were performed using 3D cultures over Matrigel in hypoxia-treated Hs578T cancer cells with diminished expression of *AFAP1-AS1*. The angiogenesis tests were conducted using human umbilical vein endothelial cells (HUVECs) and *AFAP1-AS1*- silenced Hs578T cells on 3D cell cultures. The presence of VM (CD31-/PAS+) in tumor tissues from TNBC patients with and without metastasis was assessed through immunohistochemistry using endothelial marker CD31 antibodies and periodic acid-Schiff (PAS) staining.

Results Compared with normal mammary tissues, *AFAP1-AS1* expression was higher in breast cancer tissues. Moreover, *AFAP1-AS1* expression was upregulated in the TNBC subtype compared to receptor-positive breast tumors. In addition, the expression of *AFAP1-AS1* was correlated with the expression of the thirteen genes characteristic of

*Correspondence:
César López-Camarillo
cesar.lopez@uacm.edu.mx

Full list of author information is available at the end of the article

a previously reported hypoxia signature. Interestingly, *AFAP1-AS1* was upregulated in primary TNBC tumors from patients who developed metastasis compared with the nonmetastatic group. Functional analysis revealed that the knockdown of *AFAP1-AS1* in Hs578T cells significantly impaired the hypoxia-induced VM, accompanied by a decrease in the development of 3D channel networks. Similarly, *AFAP1-AS1* knockdown counteracts the angiogenic potential of cancer cells, as indicated by a reduction in the number of polygons, sprouting cells, and nodes in HUVEC cells. Remarkably, an increase in CD31-/PAS + staining of 3D channel networks in primary breast tumors from metastatic patients was found compared with the nonmetastatic group. Finally, we found that the number of blood vessels increased in the nonmetastatic group more than in the metastatic cohort.

Conclusions Our data suggested that *AFAP1-AS1* controls both VM and angiogenesis in Hs578T breast cancer cells and that increased metastasis is associated with VM in TNBC patients.

Keywords Breast cancer, *AFAP1-AS1*, Vasculogenic mimicry, Angiogenesis, Metastasis

Background

Breast cancer (BRCA) is the most recurrent malignancy in women worldwide. Triple-negative breast cancer (TNBC) is a heterogeneous subgroup with a high proliferative and metastatic index [1]. Epidemiological evidence indicates that the 5-year disease-free and overall survival are low in TNBC patients and associated with a poor clinical response to therapy [2]. Several reports suggest that TNBC favors the generation of new blood vessels through mechanisms such as angiogenesis and, more recently, the potential of cancer cells to develop three-dimensional (3D) channel-like networks termed vasculogenic mimicry (VM). The VM process is activated mainly by a lack of oxygen and nutrients in bulk tumors' central necrotic core. Furthermore, the formation of channel networks detected through CD31 + and PAS-staining has revealed a significant presence in tumor tissues and has been associated with poor prognosis and metastatic disease [3–5].

The long non-coding RNAs (lncRNAs) are RNAs longer than 200 ribonucleotides that are generally not translated to proteins. However, recent evidence indicates that they could encode for small peptides. LncRNAs can utilize various molecular mechanisms to regulate epigenetic and transcriptional programs in cells, including decoys, guides, scaffolds, and microRNAs (miRNAs) sponges, acting as endogenous competitors [6]. Many investigations have reported that lncRNAs may act as oncogenes or tumor suppressor genes regulating essential biological functions in human cancers, such as cell proliferation, migration, invasion, metastasis, angiogenesis, and therapy responses, suggesting that they could be attractive options for targeted and personalized therapies in BRCA [6–8]. *AFAP1-AS1* is an oncogenic lncRNA that regulates the expression of various genes that impact crucial cell signaling pathways. An increase in the expression of *AFAP1-AS1* in tumor cells promotes cell proliferation, therapy resistance, and apoptosis resistance and enhances cell invasion and migration [9–11]. However, the role of this lncRNA in regulating VM and angiogenesis in TNBC patients remains poorly understood. Focusing on these facts, we decided to study the clinical and functional relevance of *AFAP1-AS1* in TNBC. The *AFAP1-AS1* expression in TCGA cancer samples was compared with those in normal tissues. In addition, the functional role of *AFAP1-AS1* in TNBC cells grown under hypoxic conditions simulating the low-oxygen levels in the inner environment of solid tumors was assessed. Finally, the presence of VM in TNBC clinical tissues from metastatic and nonmetastatic cancer patients was analyzed. Our data showed that *AFAP1-AS1* was upregulated in primary tumors from patients with metastatic disease. Moreover, it plays a vital role in regulating VM and angiogenesis, suggesting it could be a valuable therapeutic target in TNBC.

Methods

AFAP1-AS1 expression analysis in normal and BRCA patient samples

The *AFAP1-AS1* expression was evaluated in 80 and 112 normal tissues from the GTEx and TCGA datasets and compared with 1061 tumor tissues from the TCGA cohort. Additionally, the expression levels of *AFAP1-AS1* were compared between breast cancer subtypes classified according to the immunohistochemical receptor markers and the PAM50 classifier. The median expression levels were log2 transformed (TPM + 1) and were represented in scatter dot plots.

Correlation analysis between the expression of *AFAP1-AS1* with hypoxia-related genes

The relationships between *AFAP1-AS1* expression and the winter signature representative of hypoxia-related genes [25] were determined using Spearman correlation analysis. A p-value < 0.05 was considered to indicate statistical significance. Analyses were performed in Gene Expression Profiling Interactive Analysis (GEPIA2) (http://gepia2.cancer-pku.cn/#correlation).

Cell lines

HUVECs and TNBC Hs-578T cells were acquired from the American Type Culture Collection (ATCC) and cultured in Dulbecco`s Modified Eagle Medium (DMEM) supplemented with 3.7 g/L sodium bicarbonate, 10% fetal bovine serum (FBS) and penicillin and streptomycin (50 unit/mL) antibiotics (Invitrogen, Carlsbad, CA, USA) at 37 °C in a humidified atmosphere with 5% CO_2.

3D channel formation assays in 3D cell cultures

The VM was measured through the 3D channel formation in vitro. The Hs578T cancer cells (1×10^4 cells/well) were transfected with a siRNA (Thermo Fisher Scientific cat. 4390771) targeting exon 2 at the 5200-nucleotide position of the *AFAP1-AS1* sequence (60 nM) or the scramble-control (60 nM) for 48 h. Then, the transfected and untransfected control cells were cultured in a 96-well plate covered with 40 µL of Matrigel to induce the formation of 3D channels at 37 °C under normoxia or hypoxic (1% O_2) conditions for 0–9 h, as it has been well documented that hypoxia actives the 3D-channels formation in vitro and in vivo [3–8]. The formation of 3D channel networks was observed and photographed using an inverted optical microscope for 0–9 h. The data were expressed as the mean±S.D. $p<0.05$, which was considered statistically significant.

Angiogenesis assays

Hs578T breast cancer cells were cultured on 24-well plates. Once the cells reached 80% confluency, they were transfected with the siRNAs against *AFAP1-AS1* (60 nM) or scramble-control (60 nM) for 48 h. Afterward, the angiogenesis assay began with adding 50 µL of Matrigel (8 mg/mL) to 96-well plates, and the plates were incubated at 37 °C for one h. Then, HUVECs (20,000 cells/well) and Hs-578T cancer cells (20,000 cells/well) were cocultured on Matrigel in each well. Then, the plates were incubated at 37 °C for 24 h. Finally, the cells were fixed and stained with 0.5% crystal violet in a 50% ethanol/PBS mixture containing 1.25% paraformaldehyde. Images were taken with a camera attached to an inverted microscope. The following previously reported formula was used to measure the angiogenic index [12].

$$\text{Angiogenic score} = \frac{[(\text{No. sprouting cells})\,1 + (\text{No. connected cells})\,2 + (\text{Number of polygons})\,3] + [0, 1 \text{ or } 2]}{\text{Total number of cells}}$$

Patients and tissue samples

A cohort of 14 female Mexican patients diagnosed with TNBC were enrolled in the study. Of these, six patients showed metastatic disease, and eight were non-metastatic. The samples were obtained from the Regional High Specialty Hospital of Ixtapaluca with prior signed consent from the patients. This project was approved by the ethics and research committee of the Ixtapaluca Regional High Specialty Hospital (number NR-16-2020). Informed consent for study participation was obtained by all subjects or their legal guardian(s) according to local Ethic Committee. This study was performed in line with the principles of the Declaration of Helsinki.

Histological sections

With a manually rotating Spencer microtome, three sections of formalin-fixed paraffin-embedded (FFPE) tissues were obtained from each of the samples with a thickness of 3 µm. Then, samples were mounted on slides loaded with poly-L-lysine for subsequent immunohistochemistry (IHC). Three sections of 20 µm FFPE samples were obtained for RNA extraction, placed in Eppendorf tubes, and stored at -20 °C. The tonsil tissues were used as a positive control for detecting endothelial vasculature using CD31 antibodies (Sigma−Aldrich, HPA004690).

CD31 and periodic acid Schiff staining

Once 3 µm sections of tissues were obtained, the samples were rehydrated in decreasing concentrations of ethanol and water (10 min each). The slides were placed in a Coplin jar containing citrate buffer at pH 6.0 for antigen recovery. Antigen unmasking was carried out by incubating the slides at constant boiling in a citrate buffer for 20 min. The tissues were then incubated at room temperature for 30 min with 3% (v/v) hydrogen peroxide (H_2O_2) diluted in 50% methanol. To avoid nonspecific binding, a blocking solution of 1× PBS (pH 7.2), 2% FBS, and 0.5% Triton X-100 (v/v) was prepared, and 150 µL of this solution was added to each slide for 30 min at RT. The CD31 antibodies were used at a 1:200 dilution and incubated at 4 °C overnight. Two washes daily were performed with 0.1% PBS-Tween, and two were conducted with 1× PBS. A biotinylated secondary antibody (Genetex) was used at a 1:300 dilution, and the samples were incubated at 32 °C for one hour. Afterward, 3 washes were performed with PBS, and the slides were incubated with an avidin-biotin-peroxidase system (Vecta Stain ABC kit) at a 1:150 dilution at 32 °C for 30 min. A 0.04% solution of diaminobenzidine DAB was prepared in 1× PBS as a chromogen and 3% hydrogen peroxide as a substrate for the peroxidase enzyme. The chromogenic reaction was incubated for 10 min and stopped with tap water. Subsequently, the slides were incubated in 1% periodic acid for 10 min, rinsed with water, and incubated in Schiff's reagent for 10 min. The slides were washed with water and incubated with Harris hematoxylin for one minute. Finally, the tissues were dehydrated in increasing ethanol concentrations ending in 100% xylol, mounted with resin, and scanned with Aperio ImageScope Software (Leica).

Blood vessels and 3D channel networks were counted using ImageJ Fiji software.

RNA isolation from FFPE tissues

RNA was isolated from FFPE blocks using the RNeasy FFPE Kit (Qiagen) following the manufacturer's protocol. Briefly, 3 sections of 20 μm FFPE samples were used, which were dewaxed through incubation with xylol at 56 °C for 3 min. Then, PDK buffer was added, and the samples were vortexed and centrifuged at 11,000 × g/1 minute. Proteinase K was added for 15 min, and the solution was incubated for 15 min. Then, DNase enzyme was added to eliminate the genomic DNA. Finally, the RNA was purified using RNeasy MinElute columns, and 20 μl of elution buffer was added. The RNA concentration was evaluated by spectrophotometry, and RNA integrity was assessed by 1% agarose gel electrophoresis.

Quantitative RT–PCR assays

The expression levels of 10 selected lncRNAs in the Mexican cohort of TNBC patients were determined by quantitative RT–PCR with iQ SYBR Green Supermix (Bio-Rad). cDNA was synthesized from 500 ng of total RNA isolated from tumor samples embedded in FFPE using the SuperScript™ III First-Strand Synthesis System kit (Invitrogen™). The conditions were as follows: t 25 °C for 10 min., t 50 °C for 30 min and t 85 °C at 5 min. After, add 1 μL RNase H and incubated at 37 °C for 20 min. Then, the reverse transcription products were mixed with 5 μL of 2X iQ SYBR Green Supermix and 1.0 μL of forward and reverse primers (Supplementary Table1). The polymerase chain reaction was run in the Applied Biosystems QuantStudio 12 K Flex Real-Time PCR System apparatus as follows: 95 °C for 10 min, 40 cycles at 95 °C for 15 s, and 60 °C for 1 min and a hold 72° C for 30 s. The endogenous control GAPDH was used to normalize the data. The experiments were performed three times in triplicate, and the results were expressed as mean ± standard deviation. One-way ANOVA followed by Tukey's test was used to compare the means.

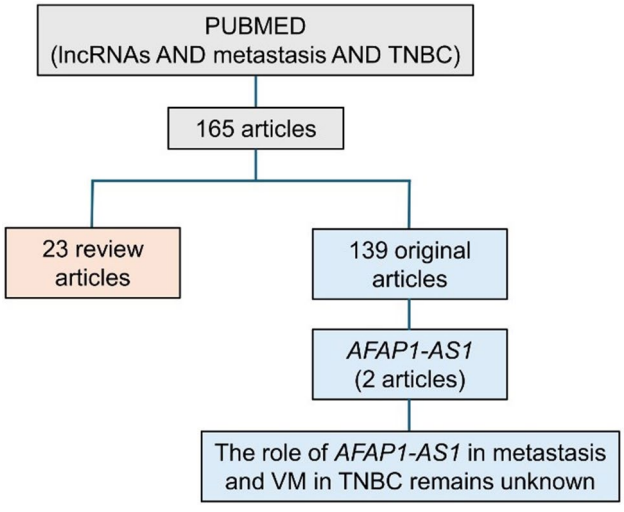

Fig. 1 Strategy to identify the lncRNAs involved in migration, invasion, and metastasis in TNBC

Statistical analysis

GraphPad Prism v8 tool was used for all the statistical analyses. The data were expressed as the means ± SDs or medians. Student's t test or the Mann–Whitney test was used to assess differences between two independent groups. Dunn's multiple comparisons test and the Kruskal–Wallis test evaluated the differences between more than two groups. P values < 0.05 were considered to indicate statistical significance for all analyses. The experiments were performed three times in triplicate, and the data were shown as the means ± S.D.s. One-way analysis of variance followed by Tukey's test was utilized to compare the differences between the means.

Results

Expression analysis of lncRNAs associated with invasion and metastasis in TNBC

Considering that the role of lncRNAs in VM and metastatic disease remains elusive, we first performed PubMed searches to identify the previously reported lncRNAs associated with metastasis and related migration and invasion processes in TNBC. The search was based on the keywords "lncRNA" AND "metastasis" AND "triple negative breast cancer" from 2012 to 2024. The query strategy and the number of identified lncRNAs are described in Fig. 1. We found 165 articles on lncRNAs associated with migration, invasion, and metastasis in TNBC. Remarkably, none of these reported lncRNAs have VM-related functions in metastatic disease. Thus, we considered initiating its characterization in TNBC patients of utmost importance.

Then, we arbitrarily selected ten metastasis and invasion-associated lncRNAs from the PubMed retrieved data (Table 1) and evaluated if they were modulated in the Mexican cohort of metastatic and nonmetastatic TNBC patients using qRT-PCR assays. Results showed that the lncRNA *CASC15* was downregulated in primary tumors from patients without metastasis. In contrast, the expression of *LUCAT1*, *TINCR-1*,*LINC00511*,*HOTAIR*,*H19*, *LINC01087*, *LINC00662*, and *CDC6-1* did not change between the two groups. Interestingly, *AFAP1-AS1* was upregulated in primary tumors from metastatic patients (Fig. 2). Therefore, we selected it for downstream analysis since its function in the metastasis process associated with VM in breast cancer is unknown.

Table 1 Ten selected lncRNAs associated with migration, invasion, and metastasis in TNBC

LncRNA	Functions in TNBC	Reference
AFAP1-AS1	AFAP1-AS1 functions in mitotic catastrophe and **metastasis** of TNBC cells by activating the PLK1 pathway.	[13]
TINCR	TINCR-miR-761 activates early TNBC **metastasis** and partially offsets luteolin's anti-tumor activity.	[14]
HOTAIR	Functions in lymph node **metastasis** and the LAR subtype of TNBC.	[16]
H19	H19 promotes TNBC cell invasion and **metastasis** through the p53/TNFAIP8 pathway.	[17]
LINC00511	The LINC00511 and miR-150/MMP13 molecules regulate cell proliferation, invasion, and **metastasis**.	[18]
LINC01087	The downregulation of LINC01087 in TNBC increases tumor aggressiveness and reduces patient survival. It controls cell proliferation, **invasion**, and drug response.	[19]
LINC00662	It is involved in cell proliferation, **migration**, and **invasion** by sequestering miR-497-5p and inducing the expression of EglN2 in TNBC cells.	[20]
lnc-CDC6-1 NONHSAT053537	It is associated with cell proliferation and **migration** by sequestering miR-215, which targets the CDC6 transcript.	[22]
LUCAT1	LncRNA LUCAT1 activates tumorigenesis and **metastasis** of TNBC by modulating the miR-5702.	[12]
CASC15	Knockdown of CASC15 inhibits cell proliferation, **invasion**, and tumor growth.	[24]

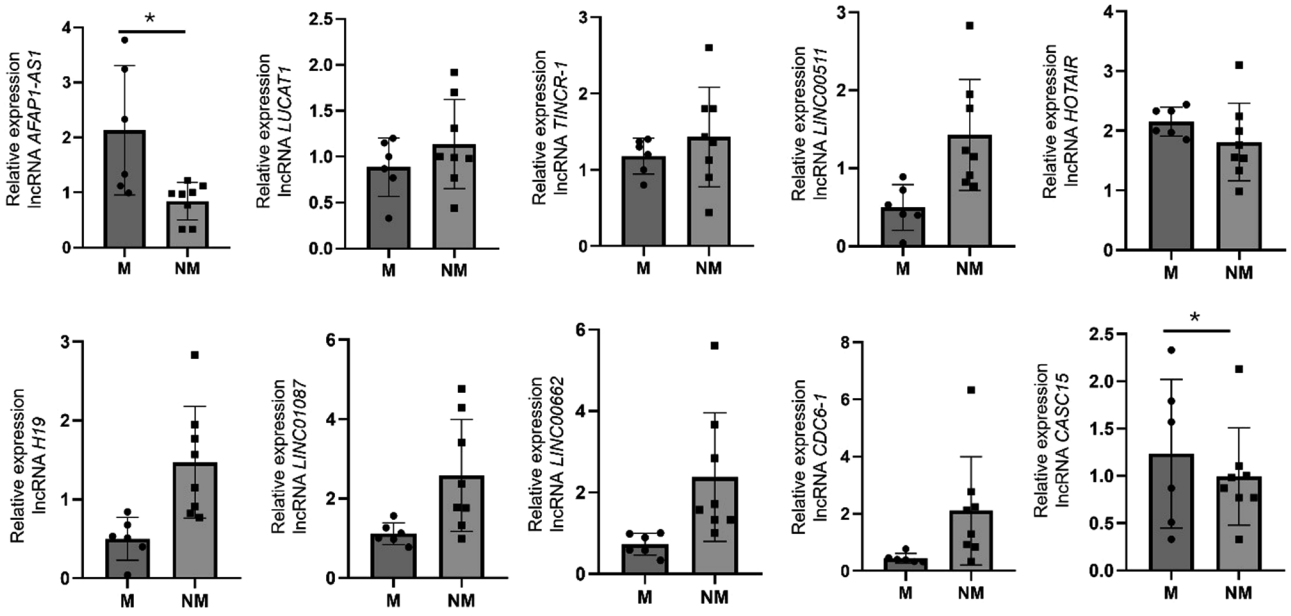

Fig. 2 Expression of lncRNAs related to metastasis in a cohort of 14 patients with TNBC with and without metastasis. qRT–PCR assays showing the differential expression of ten lncRNAs in tumor tissue from the metastatic (M) group compared with the nonmetastatic (NM) group. Experiments were performed three times in triplicate. Data were represented as mean ± S.D. One-way analysis of variance (ANOVA) followed by Tukey's test was used to compare the differences between means. A $*p<0.05$; $**p<0.01$ was considered statistically significant

AFAP1-AS1 is overexpressed in TNBC tumors and associated with a hypoxia-related gene signature

We then decided to study the expression of *AFAP1-AS1* in a more significant number of breast tumors using data from the TCGA cohort. Notably, the expression levels of *AFAP1-AS1* were greater in breast cancer tissue samples ($n=1061$) than in normal mammary tissues ($n=192$) (Fig. 3A). Among the breast cancer subtypes, the expression of *AFAP1-AS1* was significantly greater in the TNBC and basal-like molecular subtypes than in the receptor-positive luminal A/B and HER2+subtypes classified by receptors expression and PAM50 (Fig. 3B and C). Additionally, the Spearman correlation analysis revealed a significant relationship between the expression of thirteen genes of Winter's hypoxic signature (*SLC2A1*, *MRPS17*, *ADM*, *TUBB6*, *CDKN3*,*ALDOA*, *MIF*, *NDRG1*, *PGAM1*, *TPI1*, *LDHA*, *P4HA1*, and *VEGFA*) [25] with the levels of *AFAP1-AS1* in BRCA samples (Fig. 3D). To obtain more information about the probable functions of *AFAP1-AS1* in the processes related to VM and angiogenesis, we correlated its expression levels with those of vascular endothelial growth factor A (*VEGFA*), an essential gene in response to hypoxia and angiogenesis. The data showed a strong association between *AFAP1-AS1* and *VEGFA* expression (Fig. 3E).

AFAP1-AS1 silencing inhibits hypoxia-induced vasculogenic mimicry in breast cancer cells

A lack of oxygen and nutrients in the tumor microenvironment may activate VM, increasing resistance

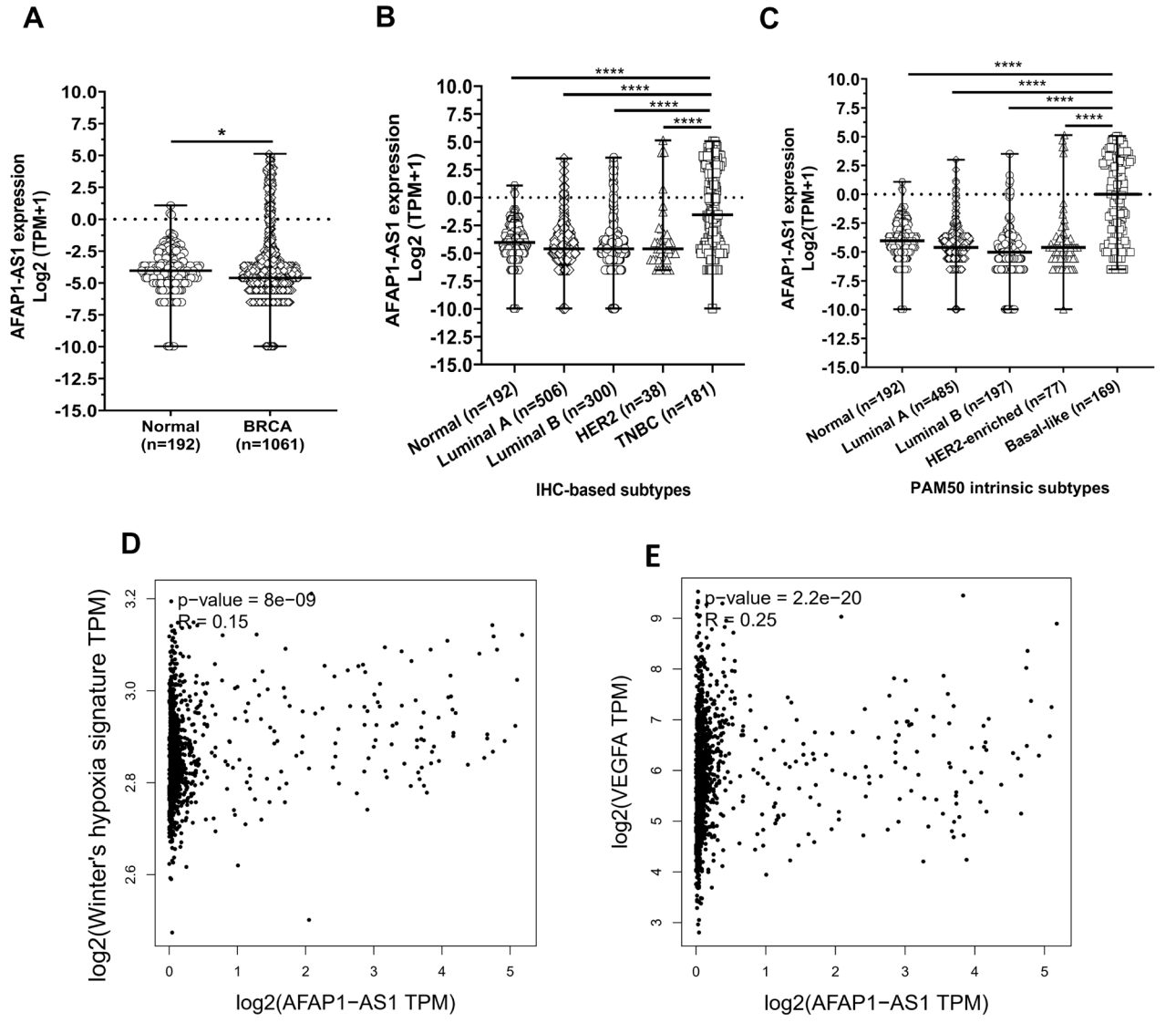

Fig. 3 AFAP1-AS1 expression is related to genes associated with the Winter hypoxia signature in BRCA samples. (**A**) *AFAP1-AS1* expression in normal tissues versus BRCA tumors. Mann–Whitney test, $*p < 0.05$. (**B**) The expression levels of *AFAP1-AS1* between the luminal, HER2+, and TNBC tumor subtypes. (**C**) *AFAP1-AS1* expression in molecular subtypes of BRCA, which were classified using the PAM50 gene signature. The scatter dot plot represents the median and range of the RNA-seq data from the BRCA-TCGA cohort. Dunn's multiple comparisons and Kruskal–Wallis tests, $****p < 0.0001$. (**D**) Thirteen genes of the Winter hypoxia signature showed a significant positive correlation with *AFAP1-AS1* expression in BRCA-TCGA tumors and normal tissue samples. (**E**) Positive correlations between *VEGFA* and *AFAP1-AS1* expression in BRCA-TCGA tumors and normal tissue samples

to antiangiogenic therapies and promoting metastasis and tumor progression [26]. We wondered whether *AFAP1-AS1* plays a role in 3D channel formation. Thus, we knocked down *AFAP1-AS1* expression in the Hs578T cancer cells and evaluated their effects on VM. The data showed that under normoxia conditions, the Hs578T cells barely developed 3D channels or bifurcation points after 3–9 h in contact with Matrigel (Fig. 4A, left panel). In contrast, under hypoxic conditions and after 3 h in contact with the Matrigel, untransfected control and scramble-control transfected cells significantly increased the formation of 3D channels and branching points, demonstrating the importance of hypoxia in the activation of VM. The number of networks increased at late incubation times (6–9 h). To confirm if *AFAP1-AS1* participates in VM, the *AFAP1-AS1*-deficient cells were treated under the same hypoxic conditions and tracked for up to 9 h. The results showed that *AFAP1-AS1* silencing significantly decreased VM development at early incubation times in Matrigel, resulting in reduced capillary-like tubes and branch points compared with untransfected control and scramble-control (Fig. 4B and C).

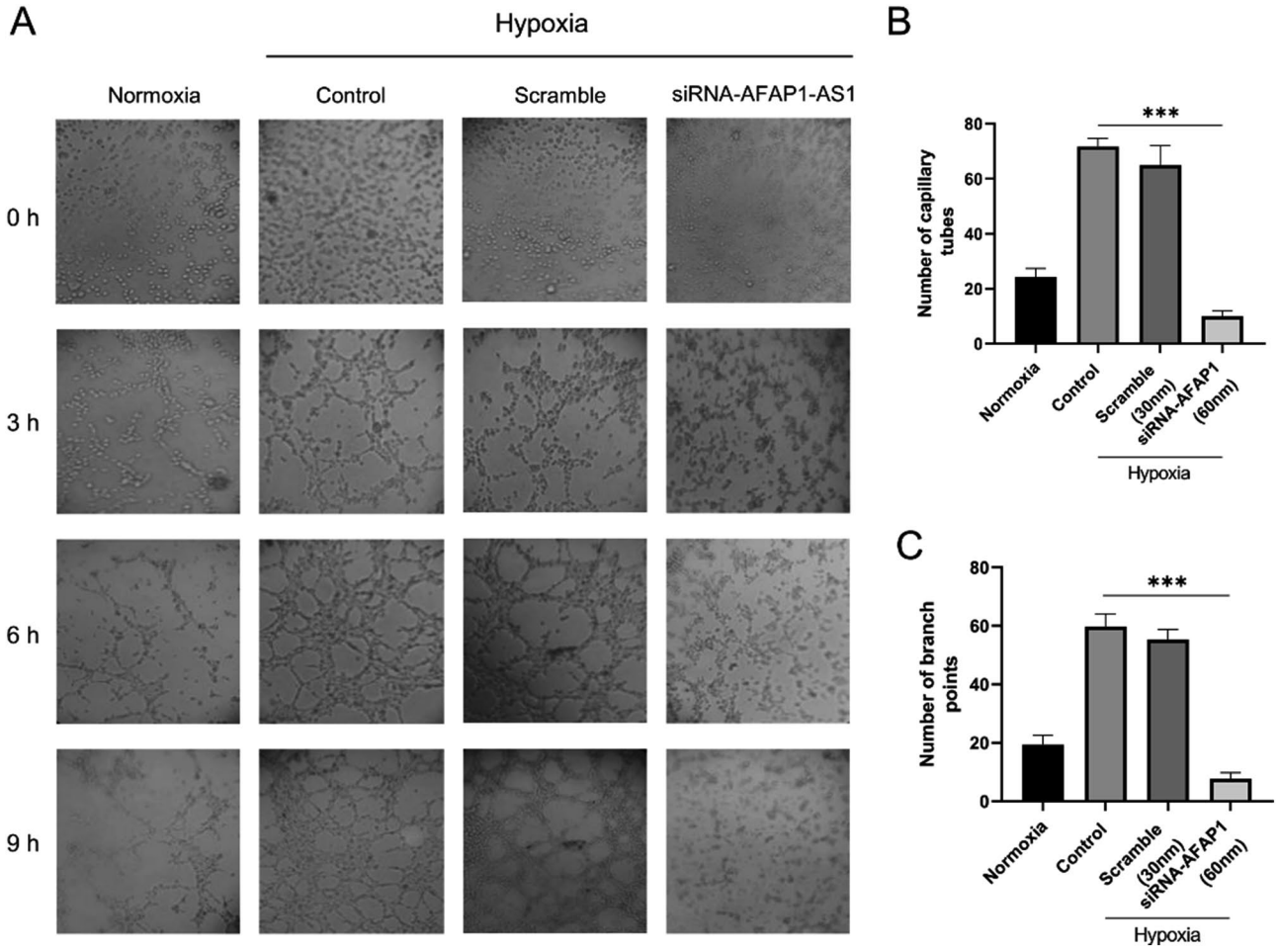

Fig. 4 Silencing of *AFAP1-AS1* inhibits vasculogenic mimicry. (**A**) Optical microscopy images of VM development in Hs578T cells grown on normoxia or hypoxia conditions. Cells were transfected with the siRNA against *AFAP1-AS1* or with the scramble-control sequence for 48 h and then tracked for channel formation during 0–9 h in Matrigel. Untransfected and scramble-transfected cells were used as controls. (**B**) Graphical representation of the number of capillary tubes and (**C**) branch points observed in panel A after 9 h of incubation on Matrigel. The assays were carried out in triplicate, and the data were expressed as the mean ± S.D. *** $p < 0.001$. Data were analyzed by one-way ANOVA. ***$p < 0.001$ was considered as statistically significant

AFAP1-AS1 controls the angiogenic potential of breast cancer cells

Next, we investigated whether *AFAP1-AS1* has a functional role in angiogenesis in TNBC cells. To test this assumption, the expression of *AFAP1-AS1* was abolished in Hs578T cells after transfection of the specific siRNA for 48 h. Scramble-control transfected cells and untransfected control Hs578T cells were used as negative controls. The results showed that coculture of untransfected or scramble-control transfected cells with HUVECs stimulated the formation of tubular-like structures (Fig. 5A-C). In contrast, the *AFAP1-AS1* knockdown significantly decreased the formation of 3D networks, followed by a significant decrease in the angiogenic index (Fig. 5D). A critical reduction in the number of tubules, polygons, connected cells, nodes, and sprouting cells affecting the reorganization of HUVECs to form tubular structures was found (Fig. 5E-J).

Identification of vasculogenic mimicry in biopsies from TNBC patients with and without metastasis

To detect the presence of 3D channels in tumor tissues from the cohort of TNBC patients with metastasis and without metastasis (Table 2), we performed immunohistochemistry assays using CD31/PAS markers. The CD31+/PAS+staining indicates the presence of blood vessels, whereas the 3D channel networks that represent VM were identified by CD31-/PAS+staining. Figure 6 shows representative images of metastatic and nonmetastatic tumor tissues stained with CD31 and PAS. Remarkably, an increase in 3D channel-like structures was found in tumor tissues from metastatic patients (Fig. 6A and B). Moreover, we detected more blood vessels in primary tumors from nonmetastatic patients than in metastatic ones (Fig. 6C and D). Additionally, we observed that erythrocytes were present within the lumen of the 3D channel-like structures. These data suggested that the

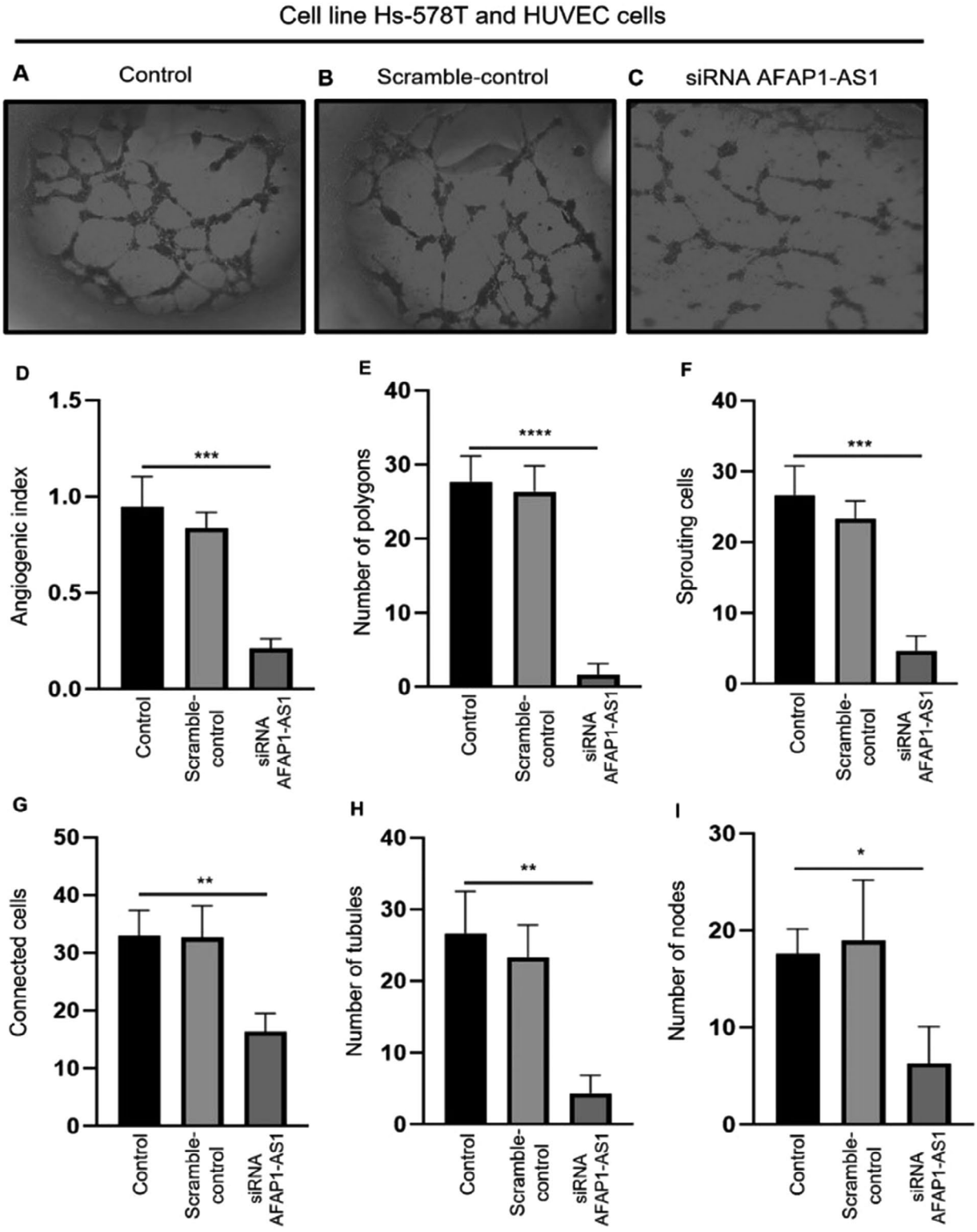

Fig. 5 *AFAP1-AS1* knockdown decreases angiogenesis in HUVECs cocultured with Hs578T cells. Assays for in vitro tube formation on Matrigel. (**A**) Control Hs578T cells. (**B**) Cells transfected with scramble-control. (**C**) Cells transfected with *AFAP1-AS1* siRNA. (**D**) Graphical representation of the angiogenic index. (**E**) Number of formed polygons. (**F**) Number of sprouted cells. (**G**) Connected cells. (**H**) Formed tubules. (**I**) Nodes. Experiments were performed three times in triplicate, and results were represented as mean ± S.D. Data were analyzed by one-way ANOVA. *$p < 0.05$; **$p < 0.01$; ***$p < 0.001$ and ****$p < 0.0001$ were considered as statistically significant

Table 2 Clinical characteristics of patients with TNBC

Clinical and pathological features	Nonmetastatic *n* = 8	Metastatic *n* = 6
Age (years)		
< 50	5	4
> 50	3	2
Triple-negative subtype	8	6
Clinical stage		
I	0	0
II	5	0
III	3	2
IV	0	4
Tumor grade		
G1	0	0
G2	3	1
G3	5	3
G4	0	2

channels could be hemodynamically functional. Interestingly, the data analysis indicated that the average number of 3D channel-like networks was increased in tumors from patients who developed metastasis (Fig. 6E), suggesting that VM promotes disease spread in TNBC patients.

Discussion

TNBC is the most aggressive subtype of BC and has a poor prognosis. Currently, the treatment options are chemotherapy, radiotherapy, and surgery. However, due to frequent metastatic events, a large percentage of these patients have a poor prognosis at the time of diagnosis [27, 28]. Therefore, the discovery of early predictive biomarkers would allow for a personalized classification to predict the tumor aggressiveness of each patient. The lncRNAs act as master regulators of the expression of various genes; therefore, it is easy to imagine that their deregulation is associated with multiple diseases, including cancer [29]. On the other hand, VM is a process that leads to resistance to therapies and favors tumor progression [26]; however, to date, very little is known about the lncRNAs involved in VM regulation in metastatic patients. Using the PubMed database, this study identified a set of lncRNAs potentially involved in VM and metastasis in TNBC. Some of these lncRNAs, such as *AFAP1-AS1* [30], HOTAIR, and TP73-AS1 in BRCA, have been associated with aggressive tumors and poor overall survival [15, 31]. We focused on the study of *AFAP1-AS1* because it has already been described in breast cancer progression [13, 32, 33]. However, its involvement in VM formation and metastasis in TNBC has not been defined. *AFAP1-AS1* expression was significantly greater

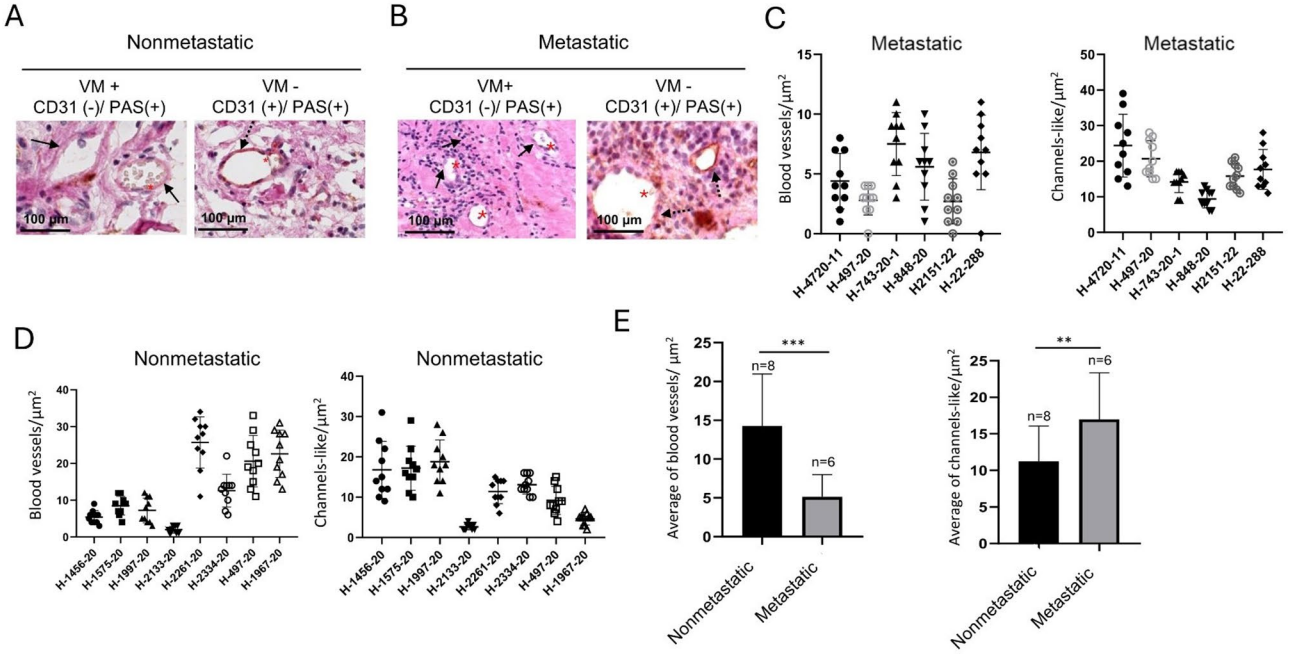

Fig. 6 Detection of 3D channels and endothelial blood vessels in metastatic and nonmetastatic tissues from TNBC patients. Representative IHC images correspond to the primary tumor tissues from (**A**) nonmetastatic and (**B**) metastatic patients. The CD31+/PAS + staining pattern denotes the blood vessels, and CD31-/PAS + indicates the channel-like networks. The black dotted arrows indicate CD31-positive endothelial cells, and the black continuous arrows indicate PAS-positive cells. Red asterisks indicate erythrocytes. Quantification of channels in tumors from (**C**) metastatic patients and (**D**) nonmetastatic patients. (**E**) Comparison of the average number of blood vessels and channels between metastatic and nonmetastatic tissues. The average number of vessels and 3D channels were determined using ImageJ Fiji tool for IHC. The results were represented as mean ± S.D. t-test (no parametric). ***$p < 0.001$ and **$p < 0.005$ was considered statistically significant

in TNBC patients than in patients with other breast cancer subtypes. Furthermore, this lncRNA was overexpressed in primary tumor tissues from metastatic TNBC patients compared to nonmetastatic patients. Previous studies have indicated that *AFAP1-AS1* expression in different tumor types is strongly associated with cellular events leading to tumor progression, such as proliferation, invasion, and metastasis [34–36]. One of the currently understudied mechanisms is VM; this event promotes the metastatic capacity in solid tumors [30]. However, no evidence showed the association between VM and metastasis by *AFAP1-AS1* in TNBC. Here, we report that decreasing *AFAP1-AS1* expression reduces VM in TNBC cells using in vitro models, a critical cellular process for growth and metastasis. We observed that all the tumors of TNBC patients were positive for VM; however, this event was more evident in the patients who presented metastasis. In a tumor context, a lack of oxygenation and nutrients leads to increased secretion of proangiogenic factors that activate endothelial cells to favor the formation of new blood vessels [37]. Studies indicate that various types of tumors present a combination of angiogenesis and VM, culminating in a poor prognosis for patients because both mechanisms operate in a coordinated manner, resulting in resistance to antiangiogenic therapies [38, 39]. Therefore, understanding the interplay between cancer cells and endothelial cells in forming closely related vascular structures may help us to identify new targets and propose strategies for TNBC therapy. Therefore, we determined that *AFAP1-AS1* promotes angiogenesis in triple-negative breast cancer cells. The results agree with those previously reported by Youwen Zhong and his collaborators, who demonstrated that the deletion of *AFAP1-AS1* inhibits angiogenesis in endometrial cancer cells [40]. The main weakness of our study is the small sample size. Thus, our findings are considered the first pilot study in breast tumor tissues since, thus far, no previous relationships between metastatic events associated with VM in breast cancer have been reported. Collectively, our data suggested that AFAP1-AS1 modulates both VM and angiogenesis in TNBC; both favor metastasis and the possibility of promoting resistance therapies.

Conclusions

In conclusion, our findings indicate that *AFAP1-AS1* plays a crucial role in VM, angiogenesis, and metastatic disease, suggesting that it could be a potential therapeutic target in TNBC.

Supplementary Information

The online version contains supplementary material available at https://doi.org/10.1186/s12885-024-13019-6.

Supplementary Material 1

Acknowledgements
We acknowledge the Universidad Autónoma de la Ciudad de México and CONAHCYT for support.

Author contributions
A.P. G.H.: Formal analysis, Investigation, Methodology, Writing – original draft. D.N. C: Formal analysis, Investigation, Methodology. Á.C.R.: conceptualization, data curation, formal analysis, investigation, methodology. M.S.M.: Investigation, Methodology, Resources. G.A.A.: Investigation, Resources. M.C.V.: Data curation, Formal analysis, Investigation. Y.P.N: Formal analysis, Investigation, Methodology. E.I.S.: Conceptualization, Formal analysis, Resources. L.A.M.: Conceptualization, Formal analysis, Writing – review & editing. C.L.C: Conceptualization, formal analysis, funding acquisition, supervision, writing – original draft, writing – review & editing.

Funding
This research was funded by Consejo Nacional de Humanidades Ciencia y Tecnologia CONAHCYT, Mexico, Grant A3-S-33674.

Data availability
All data generated or analyzed during this study are included in this published article.

Declarations

Ethics approval and consent to participate
The study protocol was approved by the ethics and research committee of the Ixtapaluca Regional High Specialty Hospital (number NR-16-2020). Written informed consent for study participation and publication of their clinical anonymized clinical data was obtained by all subjects and/or their legal guardian(s) according to local Ethic Committee. This study was performed in line with the principles of the Declaration of Helsinki.

Consent for publication
Not applicable.

Competing interests
The authors declare no competing interests.

Author details
[1]Posgrado en Ciencias Genómicas, Universidad Autónoma de la Ciudad de México, San Lorenzo 290. Col. Del Valle, Ciudad de México 03100, México
[2]Laboratorio de Onco-inmunobiologia, Instituto Nacional de Enfermedades Respiratorias "Ismael Cosío Villegas", Ciudad de México, México
[3]Unidad de Investigación en Salud del Hospital Regional de Alta Especialidad de Ixtapaluca, IMSS- Bienestar, Ixtapaluca Estado de México, Ciudad de México, México
[4]Dirección de Investigación, Hospital General de México "Dr. Eduardo Liceaga", Ciudad de México, México
[5]Laboratorio Genómica del Cáncer, Instituto Nacional de Medicina Genómica, Ciudad de México, México
[6]Departamento de Investigación, Instituto Estatal de Cancerología "Dr. Arturo Beltrán Ortega", Acapulco, Guerrero, México
[7]Programa en Biomedicina Molecular y Red de Biotecnología, Instituto Politécnico Nacional, Ciudad de México, México

Received: 18 June 2024 / Accepted: 1 October 2024
Published online: 29 October 2024

References

1. Kumar P, Aggarwal R. An overview of triple-negative breast cancer. Arch Gynecol Obstet. 2016;293(2):247–69.

2. Qiu L, Fu F, Huang M, Lin Y, Chen Y, Chen M, et al. Evaluating the Survival Benefit following ovarian function suppression in Premenopausal patients with hormone receptor positive early breast Cancer. Sci Rep. 2016;6:26627.
3. Andonegui-Elguera MA, Alfaro-Mora Y, Caceres-Gutierrez R, Caro-Sanchez CHS, Herrera LA, Diaz-Chavez J. An overview of vasculogenic mimicry in breast Cancer. Front Oncol. 2020;10:220.
4. Liu XM, Zhang QP, Mu YG, Zhang XH, Sai K, Pang JC, et al. Clinical significance of vasculogenic mimicry in human gliomas. J Neurooncol. 2011;105(2):173–9.
5. Marques Dos Reis E, Vieira Berti F. Vasculogenic Mimicry-An overview. Methods Mol Biol. 2022;2514:3–13.
6. Morales-Guadarrama G, Garcia-Becerra R, Mendez-Perez EA, Garcia-Quiroz J, Avila E, Diaz L. Vasculogenic mimicry in breast Cancer: clinical relevance and drivers. Cells. 2021;10(7).
7. Sun B, Zhang S, Zhang D, Du J, Guo H, Zhao X, et al. Vasculogenic mimicry is associated with high tumor grade, invasion and metastasis, and short survival in patients with hepatocellular carcinoma. Oncol Rep. 2006;16(4):693–8.
8. Zhang X, Zhang J, Zhou H, Fan G, Li Q. Molecular mechanisms and Anticancer therapeutic strategies in Vasculogenic Mimicry. J Cancer. 2019;10(25):6327–40.
9. Ma D, Chen C, Wu J, Wang H, Wu D. Up-regulated lncRNA AFAP1-AS1 indicates a poor prognosis and promotes carcinogenesis of breast cancer. Breast Cancer. 2019;26(1):74–83.
10. Yuan XH, Li J, Cao Y, Jie ZG, Zeng YF. Long non-coding RNA AFAP1-AS1 promotes proliferation and migration of gastric cancer by downregulating KLF2. Eur Rev Med Pharmacol Sci. 2020;24(2):673–80.
11. Xiong F, Zhu K, Deng S, Huang H, Yang L, Gong Z, et al. AFAP1-AS1: a rising star among oncogenic long non-coding RNAs. Sci China Life Sci. 2021;64(10):1602–11.
12. Aranda E, Owen GI. A semi-quantitative assay to screen for angiogenic compounds and compounds with angiogenic potential using the EA.hy926 endothelial cell line. Biol Res. 2009;42(3):377–89.
13. Cen S, Peng X, Deng J, Jin H, Deng Z, Lin X, et al. The role of AFAP1-AS1 in mitotic catastrophe and metastasis of triple-negative breast cancer cells by activating the PLK1 signaling pathway. Oncol Res. 2023;31(3):375–88.
14. Zhang ML, Liu WW, Li WD. Imbalance of Molecular Module of TINCR-miR-761 promotes the metastatic potential of early triple negative breast Cancer and partially offsets the Anti-tumor activity of Luteolin. Cancer Manag Res. 2021;13:1877–86.
15. Lozano-Romero A, Astudillo-de la Vega H, Terrones-Gurrola M, Marchat LA, Hernandez-Sotelo D, Salinas-Vera YM et al. HOX transcript antisense RNA HOTAIR abrogates vasculogenic mimicry by targeting the AngiomiR-204/FAK Axis in Triple negative breast Cancer cells. Noncoding RNA. 2020;6(2).
16. Collina F, Aquino G, Brogna M, Cipolletta S, Buonfanti G, De Laurentiis M, et al. LncRNA HOTAIR up-regulation is strongly related with lymph nodes metastasis and LAR subtype of Triple negative breast Cancer. J Cancer. 2019;10(9):2018–24.
17. Li Y, Ma HY, Hu XW, Qu YY, Wen X, Zhang Y, et al. LncRNA H19 promotes triple-negative breast cancer cells invasion and metastasis through the p53/TNFAIP8 pathway. Cancer Cell Int. 2020;20:200.
18. Shi G, Cheng Y, Zhang Y, Guo R, Li S, Hong X. Long non-coding RNA LINC00511/miR-150/MMP13 axis promotes breast cancer proliferation, migration and invasion. Biochim Biophys Acta Mol Basis Dis. 2021;1867(3):165957.
19. De Palma FDE, Del Monaco V, Pol JG, Kremer M, D'Argenio V, Stoll G, et al. The abundance of the long intergenic non-coding RNA 01087 differentiates between luminal and triple-negative breast cancers and predicts patient outcome. Pharmacol Res. 2020;161:105249.
20. Cheng L, Xing Z, Zhang P, Xu W. Long non-coding RNA LINC00662 promotes proliferation and migration of breast cancer cells via regulating the miR-497-5p/EglN2 axis. Acta Biochim Pol. 2020;67(2):229–37.
21. Jing L, Lan L, Mingxin Z, Zhaofeng Z. METTL3/LINC00662/miR-186-5p feedback loop regulates docetaxel resistance in triple negative breast cancer. Sci Rep. 2022;12(1):16715.
22. Kong X, Duan Y, Sang Y, Li Y, Zhang H, Liang Y, et al. LncRNA-CDC6 promotes breast cancer progression and function as ceRNA to target CDC6 by sponging microRNA-215. J Cell Physiol. 2019;234(6):9105–17.
23. Mou E, Wang H. LncRNA LUCAT1 facilitates tumorigenesis and metastasis of triple-negative breast cancer through modulating miR-5702. Biosci Rep. 2019;39(9).
24. Yu L, Xu Q, Yu W, Duan J, Dai G. LncRNA cancer susceptibility candidate 15 accelerates the breast cancer cells progression via miR-153-3p/KLF5 positive feedback loop. Biochem Biophys Res Commun. 2018;506(4):819–25.
25. Winter SC, Buffa FM, Silva P, Miller C, Valentine HR, Turley H, et al. Relation of a hypoxia metagene derived from head and neck cancer to prognosis of multiple cancers. Cancer Res. 2007;67(7):3441–9.
26. Wei X, Chen Y, Jiang X, Peng M, Liu Y, Mo Y, et al. Mechanisms of vasculogenic mimicry in hypoxic tumor microenvironments. Mol Cancer. 2021;20(1):7.
27. Yin L, Duan JJ, Bian XW, Yu SC. Triple-negative breast cancer molecular subtyping and treatment progress. Breast Cancer Res. 2020;22(1):61.
28. Derakhshan F, Reis-Filho JS. Pathogenesis of Triple-negative breast Cancer. Annu Rev Pathol. 2022;17:181–204.
29. Ming H, Li B, Zhou L, Goel A, Huang C. Long non-coding RNAs and cancer metastasis: molecular basis and therapeutic implications. Biochim Biophys Acta Rev Cancer. 2021;1875(2):188519.
30. Shi D, Wu F, Mu S, Hu B, Zhong B, Gao F, et al. LncRNA AFAP1-AS1 promotes tumorigenesis and epithelial-mesenchymal transition of osteosarcoma through RhoC/ROCK1/p38MAPK/Twist1 signaling pathway. J Exp Clin Cancer Res. 2019;38(1):375.
31. Tao W, Sun W, Zhu H, Zhang J. Knockdown of long non-coding RNA TP73-AS1 suppresses triple negative breast cancer cell vasculogenic mimicry by targeting miR-490-3p/TWIST1 axis. Biochem Biophys Res Commun. 2018;504(4):629–34.
32. Li F, Xian D, Huang J, Nie L, Xie T, Sun Q et al. SP1-Induced Upregulation of LncRNA AFAP1-AS1 promotes Tumor Progression in Triple-negative breast Cancer by regulating mTOR pathway. Int J Mol Sci. 2023;24(17).
33. Wu J, Xu W, Ma L, Sheng J, Ye M, Chen H, et al. Formononetin relieves the facilitating effect of lncRNA AFAP1-AS1-miR-195/miR-545 axis on progression and chemo-resistance of triple-negative breast cancer. Aging. 2021;13(14):18191–222.
34. Liu B, Jiang HY, Yuan T, Zhou WD, Xiang ZD, Jiang QQ, et al. Long non-coding RNA AFAP1-AS1 facilitates prostate Cancer progression by regulating miR-15b/IGF1R Axis. Curr Pharm Des. 2021;27(41):4261–9.
35. Fei D, Zhang X, Lu Y, Tan L, Xu M, Zhang Y. Long noncoding RNA AFAP1-AS1 promotes osteosarcoma progression by regulating miR-497/IGF1R axis. Am J Transl Res. 2020;12(5):2155–68.
36. Zhang X, Li F, Zhou Y, Mao F, Lin Y, Shen S, et al. Long noncoding RNA AFAP1-AS1 promotes tumor progression and invasion by regulating the miR-2110/Sp1 axis in triple-negative breast cancer. Cell Death Dis. 2021;12(7):627.
37. Li T, Kang G, Wang T, Huang H. Tumor angiogenesis and anti-angiogenic gene therapy for cancer. Oncol Lett. 2018;16(1):687–702.
38. Resendiz-Hernandez M, Garcia-Hernandez AP, Silva-Cazares MB, Coronado-Uribe R, Hernandez-de la Cruz ON, Arriaga-Pizano LA et al. MicroRNA-204 regulates angiogenesis and vasculogenic mimicry in CD44+/CD24- breast Cancer stem-like cells. Noncoding RNA. 2024;10(1).
39. Cannell IG, Sawicka K, Pearsall I, Wild SA, Deighton L, Pearsall SM, et al. FOXC2 promotes vasculogenic mimicry and resistance to anti-angiogenic therapy. Cell Rep. 2023;42(8):112791.
40. Zhong Y, Wang Y, Dang H, Wu X. LncRNA AFAP1-AS1 contributes to the progression of endometrial carcinoma by regulating miR-545-3p/VEGFA pathway. Mol Cell Probes. 2020;53:101606.

Publisher's note